ISBN: 978-3-95450-262-2 ISSN: 2673-5350 doi: 10.18429/JACoW-IBIC2025-MOPMO04

DIAGNOSTIC CONTRIBUTIONS TO THE COMMISSIONING OF SLS 2.0

C. Ozkan Loch†, M. Aiba, F. Armborst, M. Rey Barrera, J. Vila-Comamala,
A. Citterio, M. Dehler, A. Fazan, A. Foskolos, R. Ischebeck, J. Kallestrup, B. Keil
Paul Scherrer Institute, Villigen, Switzerland

Abstract

In January 2025, beam was first stored in the SLS 2.0, and by April 2025, the milestone of 400 mA stored beam current was reached. A variety of diagnostics were utilized to reach these milestones; for example, charge, current and loss monitors for minimizing losses and optimizing transmission and injection efficiency, polarized visible light for vertical beam size measurement, and more. This paper will highlight the contributions of the various diagnostics to the machine commissioning process.

INTRODUCTION

The Linac and Booster from the original SLS have largely been retained, except for the electron source pulser, the power supply for the booster dipole magnets [1], machine protection system [2], and some controls systems upgrades. The Booster-to-Ring Transfer Line (BRTL) and the Storage Ring (SR) injection system were completely redesigned. Several of the BRTL components and the four-kicker bump from the storage ring were inherited from the SLS.

The SLS 2.0 Storage Ring consists of 12 identical arcs with short, medium, and long straights arranged in a three-fold symmetry. There are three long straight sections. The first long straight section is dedicated to beam injection. In this injection straight, four kickers create a bump that brings the stored beam within 3 mm of the injected beam [1, 2]. The injected beam is first deflected by a permanent magnet thick septum in the BRTL, followed by a pulsed thin septum. A dedicated kicker magnet has been installed to dump the beam in a controlled manner onto a copper block upstream of the thin septum [3]. Four new 500 MHz RF cavities with Higher-Order Mode (HOM) dampers [4] are installed in sequence in a long straight section followed by horizontal and vertical collimators, while the SLS superconducting third-harmonic cavity (3HC) [5] is located in the last long straight followed by another pair of collimators.

From the Linac down to the BRTL, the existing SLS diagnostics were used. To improve injection into the Booster, beam loss monitors were added at the entrance of the Booster.

Several of the diagnostics for the BRTL and the SR were designed anew and installed at strategic locations to help commission and effectively characterize the beam parameters.

Two beamlines are dedicated to beam diagnostics, and specially developed BPM and feedback systems continuously monitor and stabilize the beam [6].

† cigdem.ozkan@psi.ch

PRINCIPLE DIAGNOSTICS

Linac to Booster Diagnostics

The available integrated current transformers from the SLS (ICTs, Bergoz instrumentation [7]) were used to measure the beam charge within the range of 100 - 500 pC, and transmission in the Linac and the Linac-to-Booster transfer line (LBTL).

The beam transmission into the Booster of 90 - 95 % was measured at 10 - 50 pC, and at high(er) charges the transmission was ~80 %.

To tune injection into the Booster and correct the beam in the first turns, turn-by-turn losses were detected using RF BPM turn-by-turn intensity readings as well as the Libera BLM system [8] to help minimize the losses. These systems were key to getting the beam into the Booster and establishing the first 100 odd turns for the RF and the ramp take over.

The injected and extracted charges at beginning and end of ramp are measured with the original SLS current monitor (MPCT). As far as upgrades to the diagnostics are concerned, the following activities were carried out: the readout of the charge monitors and current monitor in these sectors was changed to the SLS 2.0 compatible CPSI DAQ system [9], the screen monitor controls have been upgraded to the SLS 2.0 compatible motion control system, and the camera servers over Gbit links are new.

Booster to Ring Transfer Line Diagnostics

The BRTL provides the possibility for nominal injection into the SLS 2.0 SR. The purpose of the BRTL diagnostics is to support machine development with invasive screen monitors for determination of beam profiles, transverse emittance, beta-functions, dispersion and energy spread, as well as charge and loss monitors for non-invasive monitoring of transmission and injection efficiency into the SR during operation.

The ICT in the BRTL measures the transmission from the Booster to the BRTL. During the initial commissioning, the injection into the ring was established very quickly but the Booster to SR injection efficiency was limited to ~40 %.

Beam Loss Monitoring

For the commissioning and daily operation of the storage ring, loss monitors are used in the SR and the entrance of the Booster, that can detect “fast” losses from faults or beam perturbation from injection (single or turn-by-turn) and “slow” losses that influence lifetime during standard operation.

ISBN: 978-3-95450-262-2 ISSN: 2673-5350 doi: 10.18429/JACoW-IBIC2025-MOPMO04

The Libera BLMs that can detect fast losses, were placed at the Booster injection, BRTL (after septum), injection straight and collimator exits, where losses due to RF trips, emergency beam dumps, etc., are expected to be high.

For surveillance around the BRTL and SR, beam loss detectors based on a CMOS camera readout [10] are used to locate loss locations and monitor the loss pattern. The CMOS camera exposure time is set to 300 ms.

Using the CMOS BLMs, the cause of the aforementioned low injection efficiency from the Booster to the SR was identified. This limitation was primarily caused by two misaligned vacuum components: a taper element located upstream of the third-harmonic cavity and a vacuum valve right after the thin septum. The losses in the injection area were significantly reduced after the realignment of the valve in the injection straight as shown in Fig. 1. Turn-by-turn beam loss measurement with Libera BLMs was especially useful to distinguish the beam loss right after the septum exit from a possible loss after one turn. Additionally, the time between initial occurrence and recurrence of losses indicated whether the underlying mechanism was due to synchrotron or betatron oscillations.

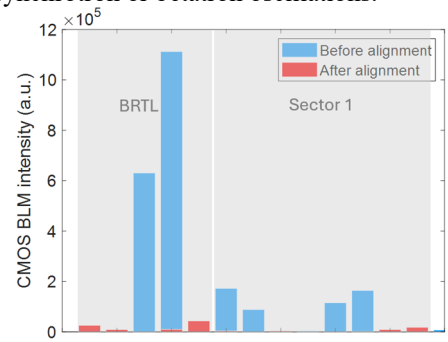

Figure 1: Change in the loss pattern in the BRTL, injection straight and Arc 01 as detected by the CMOS BLMs before (blue) and after the (orange) vacuum valve realignment.

When establishing the first turns in the ring using the turn-by-turn RF BPM position and intensity readings [11], the CMOS and Libera BLMs were helpful for tuning and minimizing losses.

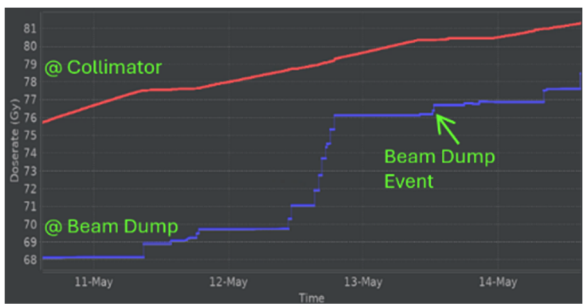

Figure 2: Dose measured by RadFETs in the collimator region and at the end of the beam dump. The dump events are seen as clear jumps in dose values at the end of the beam dump.

RadFETs [12] were installed and read out by DOSFET controllers [13] to measure the deposited doses in the following strategic locations: exit of beam dump, after and before the septum, after first permanent magnet dipole, collimators, etc. These have proven to be useful in corroborating the loss patterns detected by the other loss monitors and help track the dose distribution after every beam dump. About 1-2 Gy/day is being accumulated at the injection straight and the location of the collimators (Fig. 2), as expected. Less than 0.04 Gy/day was measured near the permanent magnets of the arcs.

Storage Ring Diagnostics

A screen monitor was designed for the new injection straight, installed at the exit of the thin final septum for injection tunings. Fig. 3 shows the injected and first turn beam seen on this monitor.

To avoid coupled bunch instabilities and to respect the impedances of the storage ring [14], an RF shield was designed and four SiC plugs were installed inside the chamber to damp the expected power on the RF shield from HOMs. The reduced heat load on the shield increased the operational lifetime of the scintillator screen—critical given that screens had previously failed within seconds of insertion at the SLS — while a measured 40 °C temperature rise in the SiC plugs verified their expected thermal performance.

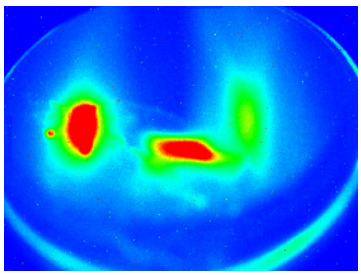

Figure 3: Injected and first turn beam seen on the screen monitor located downstream of the thin septum.

Once the first beam was successfully stored, the focus was shifted to beam-based alignment and beam optics tuning at moderate current.

Beam current is measured by two parametric current transformers (PCTs), used originally at the SLS. The nominal beam current of 400 mA was reached relatively quickly. The PCTs are also used to calibrate the BPM charge readings.

In In the following, we describe beam-size and bunch-length monitors that were also utilized to indirectly detect possible instabilities, in addition to dedicated RF BPM based systems [6].

Two front-end beamlines are dedicated to measure the electron beam by measuring the X-ray beam size using Fresnel Zone Plates (FZP) [15]. The first beamline is in a low-dispersion region to measure the horizontal emittance, and the second beamline is situated in a dispersion-dominated area to monitor the beam energy spread. Due to the mechanical aperture limitation, extraction of the visible light within the wavelength range of interest is a challenge for 4th-generation light sources. As such, the visible light from the second beamline could not be used for beam size monitoring. The first beamline has its source point in the

ISBN: 978-3-95450-262-2 ISSN: 2673-5350 doi: 10.18429/JACoW-IBIC2025-MOPMO04

first dipole after the injection straight, which has a larger extraction aperture allowing wavelengths < 500 nm.
Fresnel zone plates are used for monitoring the beam size in both planes. The setups have a single zone plate for focusing the source onto a Ce:YAG scintillator. For small beam sizes, an objective FZP is used to magnify the beam on the scintillator, as shown in Fig. 4. The exposure time was set to 5 ms for the single-zone plate, then changed to 800 ms for the two-zone setup.

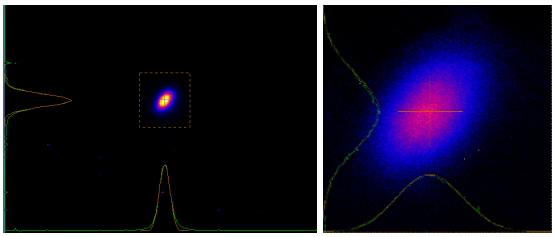

Figure 4: Beam measured with only the condenser (left; $\sigma_H \times \sigma_V = 9.8\ \mu m \times 10.5\ \mu m$) and additionally with the objective FZP (right; $10.2\ \mu m \times 10.4\ \mu m$) at 100 mA. The beam tilt is due to transverse coupling and vertical dispersion intentionally introduced to control the vertical emittance.

Visible light extracted from the emittance-dominated dipole is coupled out from the front-end into the experimental hall using two in-vacuum mirrors. Visible light was used in the first weeks of commissioning for measuring the vertical beam size using the pi-polarization [16] technique, at low currents (<50 mA).

A part of the visible light coupled out is used to measure bunch lengths with a streak camera. By monitoring few relevant bunches along the bunch train, it was possible to tune the 3HC to an optimum voltage with respect to the average bunch lengthening. One example for such a tuning exercise applied on the 3HC is shown in Fig. 5, considering the head, middle and tail bunches.

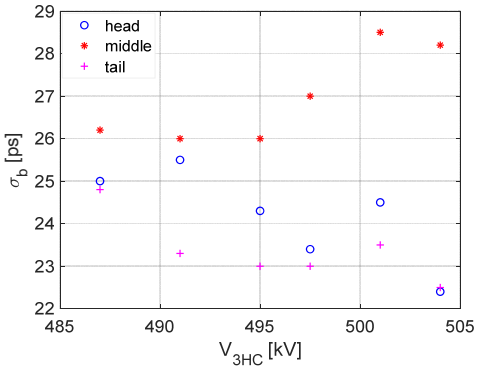

Figure 5: Bunch lengths of bunches from the head, tail, and middle part of the fill pattern (30-bucket gap) for different 3HC voltages. Optimum bunch lengthening was found at 501 kV.

SLS 2.0 operates with 480 buckets, typically utilizing a configuration with a 30-bucket gap (Fig. 6). Each filled bucket accommodates a single electron bunch, contributing to a total current of 400 mA in the storage ring. The charge per bunch is approximately 0.9 nC. A fast avalanche photodiode detects visible synchrotron radiation from the second beamline to resolve single electron bunches in each bucket of the storage ring (12 bit, ~6 GS/s) to record the filling pattern for each storage ring revolution period. The digitized waveform is obtained by applying a time interleaving scheme over consecutive revolutions (for an interleaved rate of ~96 GS/s) and is processed to calculate the amount of charge per bucket. This information is transferred via fibre link to the multi-bunch feedback system for fill pattern control [5], which also uses a complementary RF BPM based filling pattern measurements [17] that were used in the first weeks of commissioning.

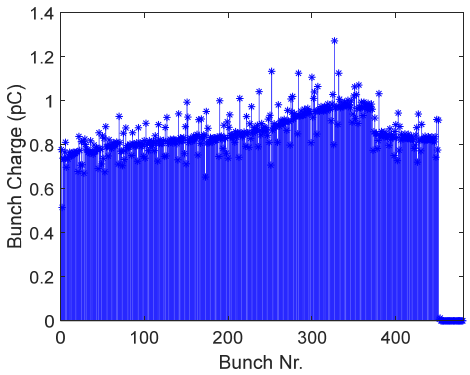

Figure 6: Fill pattern during nominal operation at 400 mA with a 30-bucket gap. The charge per bunch is calculated from PCT current readings. The filling pattern feedback loop was not closed when this data was acquired.

ACKNOWLEDGMENTS

The authors would like to thank all PSI colleagues who contributed to the realization of SLS 2.0.

REFERENCES

[1] R. Ganter, "SLS 2.0 storage ring upgrade overview", in *Proc. IPAC'25*, Taipei, Taiwan, Jun. 2025, pp. 79-82. doi:10.18429/JACoW-IPAC25-MOPB005

[2] F. Armborst, J. Kallestrup, M. I. Besana, and M. Paraliev, "SLS 2.0 machine protection", in *Proc. IPAC'23*, Venice, Italy, May 2023, pp. 1019-1022. doi:10.18429/JACoW-IPAC2023-MOPM018

[3] H. Braun *et al.*, "SLS 2.0 storage ring. Technical design report", Paul Scherrer Institut, Villigen, Switzerland, Rep. 21-02, 2021. https://www.dora.lib4ri.ch/psi/islandora/object/psi:39635

[4] F. Marhauser, E. Weihreter, D. M. Dykes, and P. A. McIntosh, "HOM Damped 500 MHz Cavity Design for 3rd Generation SR Sources", in *Proc. PAC'01*, Chicago, IL, USA, Jun. 2001, paper MPPH033, pp. 846-848.

[5] P. Bosland *et al.*, "Third Harmonic Superconducting Passive Cavities in ELETTRA and SLS", in *Proc. SRF'03*, Lübeck, Germany, Sep. 2003, paper TUO06, pp. 239-243.

[6] B. Keil *et al.*, "Overview of SLS 2.0 beam based feedbacks and BPM system", in *Proc. IBIC24*, Beijing, Sep. 2024, pp. 370-373. doi:10.18429/JACoW-IBIC2024-WEP41

[7] Bergoz instrumentation, ICT & BCM-IHR, https://www.bergoz.com/products/beam-charge-measurement/

ISBN: 978-3-95450-262-2 ISSN: 2673-5350 doi: 10.18429/JACoW-IBIC2025-MOPMO04

[8] Instrumentation Technologies, Libera BLM, https://www.i-tech.si/products/libera-blm

[9] R. Rybaniec, O. Bruendler, and B. Stef, "Real-time data acquisition with CompactPCI serial platform at PSI", in *Proc. IPAC'24*, Nashville, TN, USA, May 2024, pp. 3308-3310. doi:10.18429/JACoW-IPAC2024-THPG24

[10] C. Ozkan Loch, R. Ischebeck, and A. M. M. Stampfli, "CMOS Based Beam Loss Monitor at the SLS", in *Proc. IBIC'21*, Pohang, Korea, Sep. 2021, pp. 186-188. doi:10.18429/JACoW-IBIC2021-TUOB02

[11] B. Keil *et al.*, "Commissioning and First Operation of SLS 2.0, the Upgrade of the Swiss Light Source", Presented at IBIC'25, Liverpool, UK, Sep. 2025, paper MOCI01, this conference.

[12] RFT-300-CC10, RadFET, Oxford Scientific Products, Oxford, UK.

[13] L. Froehlich, S. Grulja, and F. Loehl, "DOSFET-L02: An Advanced Online Dosimetry System for RADFET Sensors", in *Proc. IBIC'13*, Oxford, UK, Sep. 2013, paper TUPC45, pp. 481-484.

[14] A. Citterio, M. Dehler, and L. Stingelin, "Overview of the collective effects in SLS 2.0", in *Proc. IPAC'23*, Venice, Italy, May 2023, pp. 1015-1018. doi:10.18429/JACoW-IPAC2023-MOPM017

[15] C. Ozkan Loch, M. Gregorio, R. Ischebeck, N. Samadi, and J. Vila Comamala, "Beam size measurement developments at SLS", in *Proc. IPAC'23*, Venice, Italy, May 2023, pp. 4814-4816. doi:10.18429/JACoW-IPAC2023-THPL148

[16] A. Saa Hernandez *et al.*, "The New SLS Beam Size Monitor, First Results", in *Proc. IPAC'13*, Shanghai, China, May 2013, paper MOPWA041, pp. 759-761.

[17] P. Baeta *et al.*, "First Beam Commissioning Experience With RF System On Chip Based Bunch By Bunch Signal Processing Systems at SLS 2.0", Presented at IBIC'25, Liverpool, UK, Sep. 2025, paper MOPCO12, this conference.